

## Resonance Cone Interaction With a Self-Consistent Radio-Frequency Sheath

J. R. Myra and D. A. D'Ippolito

*Lodestar Research Corporation, 2400 Central Avenue P-5, Boulder, Colorado 80301, USA*

(Received 24 July 2008; published 6 November 2008)

We study the propagation of lower-hybrid-type resonance cones in a tenuous magnetized plasma, and, in particular, their interaction with, and reflection from, the plasma sheath near a conducting wall. The sheath is modeled as a vacuum gap whose width is given by the Child-Langmuir law. The application of interest is when the resonance cones are launched (parasitically) by an ion-cyclotron radio-frequency antenna in a typical rf-heated tokamak fusion experiment. We calculate the fraction of launched voltage in the resonance cones that is transmitted to the sheath, and show that it has a sensitive thresholdlike turn on when a critical parameter reaches order unity. Above threshold, the fractional voltage transmitted to the sheath is order unity, leading to strong and potentially deleterious rf-wall interactions in tokamak rf heating experiments. Below threshold, these interactions can be avoided.

DOI: 10.1103/PhysRevLett.101.195004

PACS numbers: 52.35.Mw, 52.40.Kh, 52.50.Qt, 52.55.Fa

Fascinating wave-propagation phenomena can occur in media which have an anisotropic dielectric tensor especially when its principle components have differing signs. In the latter case, considering waves of fixed frequency  $\omega$ , the spatial wave-propagation operator becomes hyperbolic instead of elliptical leading to the formation of resonance cones (RCs). In three dimensions, waves launched from a point source will propagate in trajectories that lie on the surface of a cone with the source located at the point of the cone. These localized structures are in sharp contrast to the usual situation where a point source leads to wave fronts that spread due to diffraction and dispersion.

RCs have been known for many decades. They were first measured by Fisher and Gould [1] and subsequently studied by many authors (see, e.g., Refs. [2–4]). In magnetized plasmas, the necessary conditions on the dielectric occur naturally in several wave-propagation regimes, including upper- and lower-hybrid RCs and Alfvén RCs. An excellent overview is given by Bellan [5], and additional background may be found in Stix [6]. In addition to plasma applications, RCs have also been investigated in metamaterials [7] where there may be interesting practical applications.

In this Letter, our main interest is in application of RC phenomena to high-power heating experiments in fusion-relevant plasmas—in particular ion-cyclotron range of frequencies and lower-hybrid heating experiments in tokamaks. Waveguides or antennas launch the rf waves in the tenuous edge plasma. Wave propagation is dominantly inwards, towards the core region, where the waves are usually employed for heating and/or driving currents. Strong, and potentially deleterious, interactions of the launched waves sometimes occur in the tenuous edge region, sapping the launched wave of power and causing unwanted impurity sputtering and outgassing from the vessel “walls” or plasma-limiting surfaces [8]. We will

show that RCs provide a plausible mechanism for transporting strong localized rf voltages to rf sheaths at the wall.

For ion-cyclotron range of frequencies heating, the antenna is designed to primarily launch the fast Alfvén wave. However, due to the rotational transform in the tokamak, which causes a field line tilt at the antenna relative to the toroidal direction, fast wave antennas in practice always couple to the slow wave as well. Other geometrical and electromagnetic effects enhance this unwanted coupling [9], which may launch RCs in the tenuous plasma of the far scrape-off layer, e.g., between antenna limiters, or from slots that are frequently found in the sides of the antenna.

To describe the slow wave propagation, we define a tenuous plasma by the condition that the local plasma density be small compared with the lower-hybrid density, defined by  $\omega^2 = \omega_{pi}^2 + \Omega_i^2$  where  $\omega_{pi}$  and  $\Omega_i$  are the ion plasma and ion-cyclotron frequencies, respectively. In the tenuous plasma limit, treated herein, the plasma dielectric tensor is given by

$$\vec{\epsilon} = (\vec{\mathbf{I}} - \mathbf{b}\mathbf{b}) + \mathbf{b}\mathbf{b}\epsilon_{\parallel}, \quad (1)$$

where  $\epsilon_{\parallel} = 1 - \omega_{pe}^2/\omega^2 \approx -\omega_{pe}^2/\omega^2$  and  $\mathbf{b} = \mathbf{e}_z$  is the direction of the background magnetic field. For simplicity we consider here the 2D (line source) problem with  $y$  ignorable. The RC source is taken to be a localized Gaussian in  $z$  and we follow propagation in the direction of increasing  $x$ .

The electrostatic dispersion relation takes the form

$$k_x = -(\omega_{pe}/\omega)|k_z|, \quad (2)$$

where the choice of signs insures outgoing wave energy propagation for this backward propagating mode ( $v_{ph}v_g < 0$ ). The 2D resonance cone solution is given by  $\Phi = f(\xi \pm z)$  where  $\xi = (\omega_{pe}/\omega)x$  and  $f$  is an arbitrary localized (e.g., delta) function.

In the electromagnetic case, the slow wave dispersion relation is

$$n_x^2 = -\varepsilon_{\parallel}(n_z^2 - 1), \quad (3)$$

where  $n = kc/\omega$ , and RC behavior occurs for  $n_z > 1$ . In the opposite limit, the waves are evanescent on the scale  $\delta_e = c/\omega_{pe}$ . An example of RC propagation is shown in Fig. 1.

It is straightforward to construct an analytical solution for the interaction of the electrostatic RC with an ideal perfectly conducting or perfectly insulating boundary, using the method of images. For the conducting case (boundary condition  $\Phi = 0$  at  $z = 0$ ), if the incident wave is  $f(\xi + z)$  then the total solution is  $f(\xi + z) - f(\xi - z)$ , so there is reflection with a phase shift. In the insulating case (boundary condition  $\partial\Phi/\partial z = 0$ ), the solution is  $f(\xi - z) + f(\xi + z)$ . In the following, we first develop the method of images for the general electromagnetic case with sheath boundary conditions

$$E_x - \sigma \partial_x \Delta \varepsilon_{\parallel} E_z = 0, \quad (4)$$

where the sheath is modeled as a thin vacuum layer of width  $\Delta$  adjacent to the metal surface,  $\sigma = \mathbf{s} \cdot \mathbf{e}_z$ , and  $\mathbf{s}$  is the unit surface normal pointing into the plasma [10]. This model provides a zero-order description of the effects of sheaths on rf waves, because the main property of the sheaths is the exclusion of electrons from the sheath layer, and this effect is felt most dramatically through the local reduction in  $\varepsilon_{\parallel}$ .

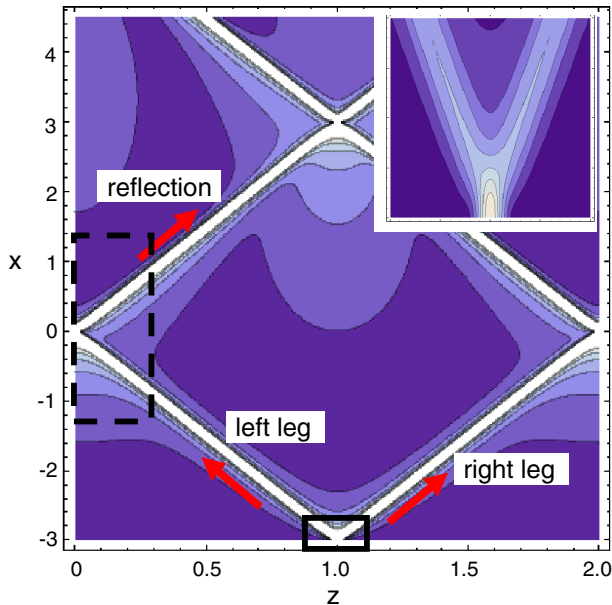


FIG. 1 (color online). Resonance cone propagation from a localized source at  $x = -3$ ,  $z = 1$  in the plane  $z/L$  and  $x/\delta_e$  with walls at  $z = 0, 2$ . Inset shows the launch region. Energy propagates to increasing  $x$ . Dotted region is the domain of the analytical calculation.

The slow wave polarization is given by  $E_x = GE_z$  where  $G = n_x n_z / (n_z^2 - 1)$ . Because in general the dispersion relation and boundary conditions are not linear in  $k_x$  and  $k_z$ , the method of images must be applied in Fourier space to each mode. The solution arises from a superposition of a source  $S(k_z)$  and an image source  $A(k_z)S(-k_z)$  which creates the reflection, where  $A$  is determined by the boundary condition. The desired solution takes the form (for the wall at  $z = 0$ , hence  $\sigma = 1$ )

$$E_z = \int_{-\infty}^{\infty} \frac{dk_z}{2\pi} e^{ik_x x + ik_z z} \left( S(k_z) - \frac{G(-k_z) - ik_x \Delta \varepsilon_{\parallel}}{G(k_z) - ik_x \Delta \varepsilon_{\parallel}} S(-k_z) \right), \quad (5)$$

where  $S(k_z)$  is the Fourier transform of the source function  $S(z)$ . We now choose  $S(z)$  to describe a single leg of a left-going RC launched from a Gaussian source far from the wall (see Figs. 1 and 2)

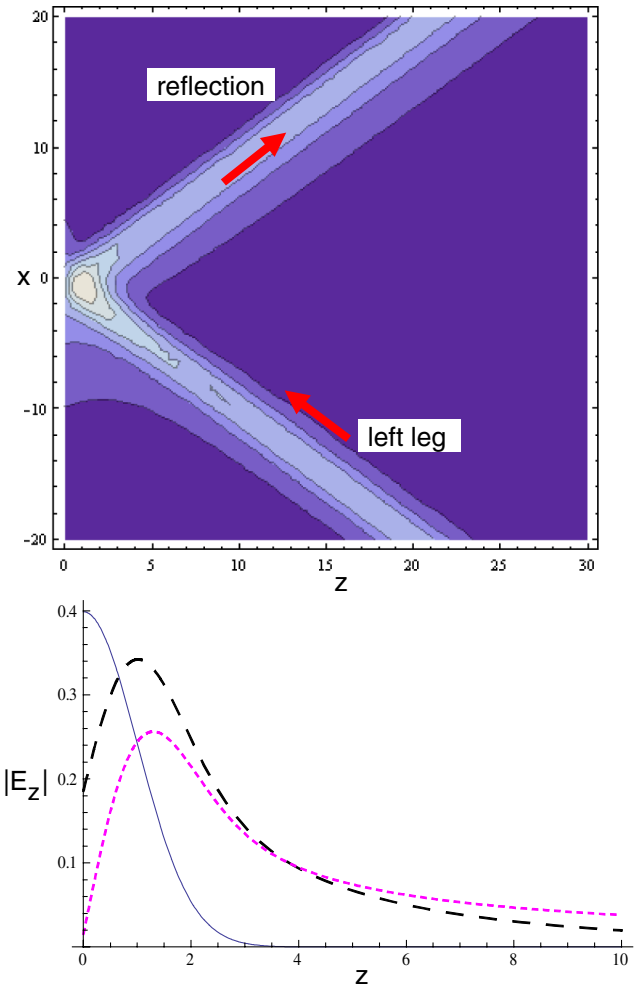


FIG. 2 (color online). Top: Resonance cone interaction with a sheath at  $x = z = 0$  for  $\Lambda = 3$ . Bottom:  $|E_z(z)|$  at  $x = 0$  for the cases  $\Lambda = 0$  (blue solid line), 3 (black dashed line), and 100 (magenta dotted line). See following Eq. (8) for definitions of dimensionless  $x$  and  $z$ .

$$S(k_z) = -V_0 \Theta(-k_z) e^{-k_z^2 a^2/2 - ik_z z_0 + ik_x x_0}, \quad (6)$$

where  $\Theta$  is the Heaviside step function,  $a \ll z_0$  is the Gaussian width in  $z$ , and we choose the launch point  $x = x_0$ ,  $z = z_0$  such that the  $x_0$  and  $z_0$  terms in Eq. (6) cancel. (The image source is at  $x = x_0$ ,  $z = -z_0$ .) Then the wall interaction occurs at  $x = z = 0$ .

Near the source launch point, where only the  $S(k_z)$  term need be retained in Eq. (5), the Fourier transform may be inverted to obtain the source fields in terms of error functions. The voltage launched into the left-going RC is obtained as  $V^{(L)} = -\int dz E_z^{(L)}(x = x_0) = V_0/2$ ; i.e., the normalized Gaussian source provides a voltage drop of  $V_0$ , half of which is carried away in each cone.

Taking the *electrostatic limit* of Eq. (5), and using the dispersion relation, the Fourier transform may be inverted to yield

$$\frac{aE_z}{V_0} = -\int_0^\infty \frac{dp}{2\pi} e^{-p^2/2 - ip\hat{x}} \left( e^{-ip\hat{z}} + \frac{1 - ip\Lambda}{1 + ip\Lambda} e^{ip\hat{z}} \right), \quad (7)$$

where

$$\Lambda = -\frac{\Delta \varepsilon_{\parallel}}{a} \quad (8)$$

and  $\hat{x} = (\omega_p/\omega)x/a$ ,  $\hat{z} = z/a$ .  $\Lambda$  is the fundamental parameter governing RC sheath interactions. The limit  $\Lambda = 0$  ( $\infty$ ) corresponds to the conducting (insulating) limit.

Figure 2 illustrates the wave patterns resulting from Eq. (7) for the case where the RC impacts the wall from the right. Depending on  $\Lambda$ , there are differences in the details of the solution, but lossless reflection which leaves the RC intact as a localized structure always occurs.

The sheath and plasma voltage drops are readily calculated from Eq. (7). The sheath voltage is defined as

$$V_{\text{sh}} = -\Delta \varepsilon_{\parallel} E_z(z = 0), \quad (9)$$

which is consistent with the integrated  $E_z$  across the vacuum layer of width  $\Delta$ , taking into account that  $E_z$  in the sheath matches  $\varepsilon_{\parallel} E_z(z = 0)$  in the plasma [10]. The sheath voltage  $V_{\text{sh}}$  at the location of the RC-wall interaction ( $x = z = 0$ ) is

$$\frac{V_{\text{sh}}}{V_0} = \frac{-\Lambda}{\pi} \int_0^\infty dp \frac{e^{-p^2/2}}{1 + ip\Lambda} \equiv f(\Lambda). \quad (10)$$

The plasma voltage drop at this  $x$  location is

$$V_p = -\int_0^\infty dz E_z(x = 0). \quad (11)$$

Using  $(1 - ip\Lambda)/(1 + ip\Lambda) = 1 - 2ip\Lambda/(1 + ip\Lambda)$  in Eq. (7), it can be shown that

$$V_p + V_{\text{sh}} = \frac{1}{2} V_0; \quad (12)$$

thus the launched voltage is split between the plasma and

the sheath. However, we shall see that  $|V_{\text{sh}}|$  can exceed  $|V_0/2|$ .

The function  $f(\Lambda)$  is expressible in terms of error and gamma functions; however, in practice it is simplest to compute it numerically. It has the asymptotic forms

$$f(\Lambda) \sim \begin{cases} -\Lambda/(2\pi)^{1/2} & \Lambda \ll 1 \\ C_0 + (i/\pi) \ln \Lambda & \Lambda \gg 1, \end{cases} \quad (13)$$

where  $C_0 = -1/2 - i/(2\pi)(\gamma_E - \ln 2)$  and  $\gamma_E$  is Euler's constant. In particular  $|f(\Lambda)|$  is monotonically increasing from zero at  $\Lambda = 0$ .

In reality,  $\Lambda$  cannot be specified *a priori*, because the sheath width  $\Delta$  depends on the strength of the rf fields, through the Child-Langmuir law. In the high-voltage limit the rf voltage across the sheath entrance  $V_{\text{sh}}$  and sheath width are related by

$$\Delta = \lambda_{\text{de}} \left| \frac{\alpha e V_{\text{sh}}}{T} \right|^{3/4}, \quad (14)$$

where  $\alpha$  is a numerical factor of order unity, and we assume  $|eV_{\text{sh}}/T_e| \gg 1$  [9]. Thus the self-consistent value of  $\Lambda$  must satisfy

$$\left( \frac{\Lambda}{\Lambda_0} \right)^{4/3} = |f(\Lambda)|, \quad (15)$$

where  $\Lambda_0$  is a reference value defined by

$$\Lambda_0 = -\frac{\lambda_{\text{de}} \varepsilon_{\parallel}}{a} \left| \frac{\alpha e V_0}{T} \right|^{3/4}. \quad (16)$$

Solving Eq. (15) in the small and large argument limits and computing the resulting self-consistent sheath voltage yields

$$\left| \frac{V_{\text{sh}}}{V_0} \right| = \begin{cases} \Lambda_0^4/(2\pi)^2 & \Lambda_0 \ll 1 \\ |C_0 + (i/\pi) \ln \Lambda| & \Lambda_0 \gg 1. \end{cases} \quad (17)$$

The general result is illustrated in Fig. 3.

There is practically no voltage across the sheath for  $\Lambda_0 < 1$ . This is evident both from Fig. 3, and also from the analytical result that  $|V_{\text{sh}}/V_0| \sim 0.025\Lambda_0^4$  which is small due to both the high power of  $\Lambda_0$  and the small coefficient. On the other hand, for  $\Lambda_0 > 4$  or so, an order unity fraction of the launched voltage appears across the sheath. Thus, roughly speaking,  $\Lambda_0 \sim 4$  is a threshold value demarcating a region where the RC voltage launched from the antenna ends up being transmitted efficiently to the sheath. Since the launched RC voltage is expected to be large ( $V_0 \gg T_e/e$ ) for high-power antennas, this is equivalent to saying that  $\Lambda_0 \sim 4$  demarcates the region of strong antenna-wall coupling. Physically, a strong interaction arises when a large  $E_{\parallel}$  is present at the plasma boundary because  $\Delta$  depends nonlinearly on  $V_{\text{sh}}$  through the Child-Langmuir law, Eq. (14).

For application to experiments, we assume that the RC voltage is comparable to the voltage on antenna sheaths, or the voltage induced along field lines near the antenna

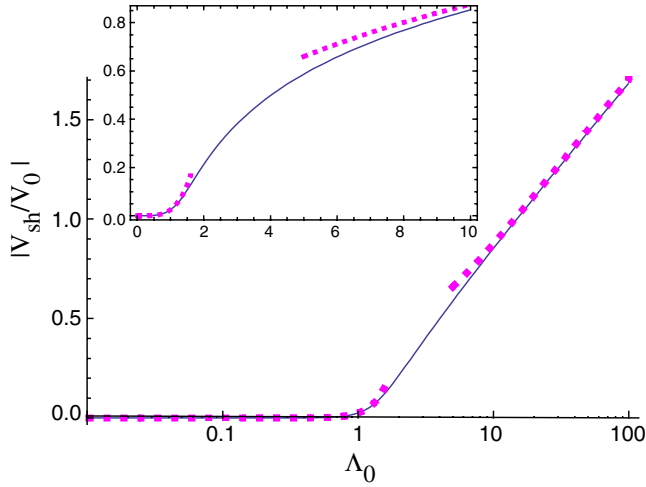


FIG. 3 (color online). Self-consistent sheath voltage on a log scale and (inset) linear scale for  $\Lambda_0 < 10$ . The solid blue line is the numerical result and the magenta dots are the asymptotic results. Note the different scales for both axes in the inset.

structure, viz., typically a few hundred volts. For illustrative parameters (e.g., for the far scrapeoff layer of Alcator C-Mod,  $T_e = 10$  eV,  $\alpha = 0.6$ ,  $B = 5.3$  T,  $\omega/2\pi = 80$  MHz,  $V_0 = 200$  V,  $n = 1 \times 10^{11}$  cm $^{-3}$ ), we find from Eq. (16) that  $\Lambda_0 > 4$  occurs when structures are launched with parallel scale  $a < 15$  cm, i.e.,  $E_{\parallel} > 13$  V/cm. Since the RC propagates nearly parallel to  $B$  ( $\Delta x/\Delta z \sim \omega/\omega_{pe} \ll 1$ ) this mechanism could plausibly explain rf interaction with vessel surfaces in Alcator C-Mod [11,12]. For larger  $V_0$  and/or smaller  $a$  the voltage appearing on the wall sheaths will be of order  $V_0$ . Conversely, reducing  $V_0$  or increasing  $a$  should result in a dramatic reduction in deleterious rf interactions with the wall, since below the threshold, the RCs do not transmit the antenna voltage  $V_0$  to the wall.

In principle, other nonlinear effects may coexist with sheath formation. For the parameters of our example, it can be shown that  $k_{\parallel}v_e/\omega$ ,  $k_{\parallel}\xi_{e\parallel} \ll 1$  where  $\xi_{e\parallel}$  is the characteristic electron jitter excursion distance; thus, neither Landau interactions nor stochastic electron heating should

be important. For the ions,  $k_{\perp}\rho_i$ ,  $k_{\perp}\xi_{i\perp} \ll 1$  so ion trapping is not expected, unless a cyclotron resonance ( $\omega \approx n\Omega_i$ ) is present [13]. Finally,  $\psi_p/T < 1$  where  $\psi_p$  is the ponderomotive potential. This excludes strong ponderomotive expulsion for these parameters; however, at lower frequencies or stronger rf fields, it could be significant, possibly allowing the RCs to dig a low density channel for their own propagation.

We thank the RF SciDAC and Alcator C-Mod teams for stimulating discussions. This work was supported by U.S. DOE Grants DE-FG02-97ER54392 and DE-FC02-05ER54823.

- 
- [1] R. K. Fisher and R. W. Gould, Phys. Rev. Lett. **22**, 1093 (1969).
  - [2] P. Bellan and M. Porkolab, Phys. Fluids **17**, 1592 (1974).
  - [3] K. H. Burrell, Phys. Fluids **18**, 897 (1975).
  - [4] T. Ohnuma, T. Kuwabara, K. Shibata, and S. Adachi, Phys. Rev. Lett. **37**, 206 (1976).
  - [5] P. M. Bellan, in *Fundamentals of Plasma Physics* (Cambridge University Press, Cambridge, England, 2006).
  - [6] T. H. Stix, in *Waves in Plasmas* (Springer-Verlag, New York, 1992).
  - [7] K. G. Balmann, A. E. Lüttgen, and P. C. Kremer, IEEE Antennas Wireless Propag. Lett. **1**, 146 (2002).
  - [8] J.-M. Noterdaeme and G. Van Oost, Plasma Phys. Controlled Fusion **35**, 1481 (1993), and references therein.
  - [9] J. R. Myra, D. A. D'Ippolito, D. A. Russell, L. A. Berry, E. F. Jaeger, and M. D. Carter, Nucl. Fusion **46**, S455 (2006), and references therein.
  - [10] D. A. D'Ippolito and J. R. Myra, Phys. Plasmas **13**, 102508 (2006); see also the appendix of J. R. Myra *et al.*, Phys. Plasmas **1**, 2890 (1994).
  - [11] S. J. Wukitch *et al.*, in *Proceedings of the 21st IAEA Fusion Energy Conference, Chengdu, 2006* (IAEA, Vienna, 2007), paper IAEA-CN-149-FT/1-6.
  - [12] B. Lipschultz, D. A. Pappas, B. LaBombard, J. E. Rice, D. Smith, and S. J. Wukitch, Nucl. Fusion **41**, 585 (2001).
  - [13] S. J. Karttunen *et al.*, in *Proceedings of the 14th International Conference on Plasma Physics and Controlled Nuclear Fusion Research, Wurzburg, 1992* (IAEA, Vienna, 1993), paper IAEA-CN-56/E-3-2, p. 711.